

Microbial Fuel Cell Optimization System Model

Synopsis

In this section of our project we will present and assess the viability of our model utilizing computational methods to unravel the genetic networks involved in our experimental design. The medium we utilized to perform our computational assessment is the technical computing language of Matlab. In the past few years Matlab's 'Simbiology' package utilizing has been growing among scientists seeking to generate mathematical models for cell biology. Therefore, our approach took the initiative to utilize the package to characterize the interactions of our bio bricks with other cellular components.

In order to model our gene network we employed the power of Ordinary Differential Equations (ODE). In each paradigm of reactivity between reactants and products the ODE's were optimized to characterize the functional connectivity between our bio bricks. Here we present in detail the network diagrams, the output of our functions, and the methodology utilized to generate abstract plots of the outputs of our networks.

The two networks we are presenting involve the function generated within a single E. Coli bacterium, upon transfection of the plasmids described in our bio brick section. The first network is that of Proteorhodopsin, a light-driven proton pump, allowing for generation of ATP and proton output that would lead to an increased efficiency of the Microbial Fuel Cell. The second network involves the functionality of NADH oxidase, in inducing an anaerobic environment, and through its biochemical reactivity increase electricity generation by the Microbial Fuel Cell system.

Differential Equation Approach

To generate the model we had to utilize a mathematical approach that would be able to characterize the following biochemical processes.

Table 1: Process Characterization

RNA Transcription
RNA Degradation
Protein Translation / Synthesis
Protein Degradation
Enzyme Driven Reactions
Protein-Protein Interactions
Pump-Mediated Transport
Molecule/ Ion Diffusion

To achieve such a challenging task we employed the strategies concerning characterization by differential equations described in “Computational Modeling of Genetic and Biochemical Networks” by James M. Bower and Hamid Bolouri. By determining the applicability of reaction orders we optimized our functions to determine the desired output, as describe for each process below.

RNA Transcription and Degradation

In the model described in the following sections we utilized the following general function to determine the RNA transcription and Degradation.

$$f_{RNA}(t) = \frac{d[RNA]}{dt} = K_f[DNA] - K_d[RNA]$$

,where [RNA] and [DNA] is the molecule number of nucleic acids present at time $t=t_x$, K_f is the synthesis rate and K_d is the degradation rate of RNA respectively.

Protein Translation and Degradation

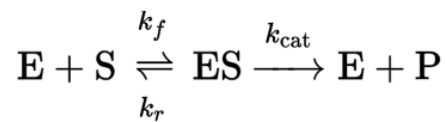
To model the translation and degradation of protein molecules involved in our model we utilized the general expression below.

$$f_{Protein}(t) = \frac{d[Protein]}{dt} = K_f[RNA] - K_d[Protein]$$

,where [RNA] and [Protein] is the molecule number of nucleic acids and amino acids present at time $t=t_x$, K_f is the synthesis rate and K_d is the degradation rate of Protein respectively.

Enzyme Driven Reactions

Given a reaction that utilizes enzyme catalysis given by the chemical equation below we can deduce the kinetics by utilizing mass-action ODE.



, where E is the amount of Enzyme, S the amount of Substrate, ES the complex of the previous elements, P the product of the catalysis, K_f the rate of complexion synthesis, K_r the rate of complexion reversal and K_{cat} the rate of catalysis

The rates for such reactions are given by the following expression.

$$f_{catalysis}(t) = \frac{d[Product]}{dt} = K_{cat}[Enzyme \cdot Substrate]$$

Protein-Protein Interactions

In the subsequent sections of the model we utilize protein-protein interactions to mainly described complex formation among a pair of proteins. Such a process is described by the general function below.

$$f_{complexing}(t) = \frac{d[Protein_x \cdot Protein_y]}{dt} = K_{complexing}[Protein_x][Protein_y] - K_{dissociation}[Protein_x \cdot Protein_y]$$

,where $[Protein_x \cdot Protein_y]$ stands for the number of complexes, $[Protein_x][Protein_y]$ for the number of molecules of protein x and protein y, $K_{complexing}$ for the rate of binding and $K_{dissociation}$ for the rate of dissociation between protein x and y.

Molecule/Ion diffusion

Molecular diffusion across the membrane was characterized by the following function.

$$f_{diffusion}(t) = \frac{d[Diffusion]}{dt} = K_{introduction}[Unit] - K_{expulsion}[Unit]$$

, where $d[Diffusion]/dt$ is the change between intracellular and extracellular number of units at time $t=t_x$, $[Unit]$ is the number of molecules/ions present at the intracellular or extracellular environment, $K_{introduction}$ and $K_{expulsion}$ are the rates of intracellular diffusion and extracellular diffusion.

Rate Constant Estimation

In this section we will describe the approach utilized to generate the rate of reaction for general processes utilized in our model and thereafter show how those statements were introduced in the model. The most convenient and robust resource we utilized in this estimation was the “Bio Numbers” database produced by Harvard University (<http://bionumbers.hms.harvard.edu>).

Rate of RNA Transcription and Degradation

By utilizing the database and assuming that our E. Coli would be grown under a environment of medial growth we estimated that the rate of transcription of RNA would be approximately 70 nucleotides per second. Therefore, by assuming that the only variable among bio brick transcription would be the length of the transcribed sequence we generated the following general expression for transcription. This normalization was performed to establish the rate constant for production of a single molecular unit of nucleic acid.

$$K_{\text{transcription}} = \frac{[\text{Length of Transcript}] \text{ nts}}{\frac{[\text{Rate of Transcription}] \text{ nts}}{\text{second}}} = \frac{[\text{Length of Transcript}]}{70} \text{ second}$$

In the other hand to estimate the rate of RNA degradation we again harvested from the database that the usual RNA half-life for E. Coli ranges from 20-40 minutes. Therefore, we assumed an average half-life of 30 minutes or for our purposes 1800 seconds. Next, assuming first-order kinetics for degradation we utilized the half-life expression to calculate the rate of the degradation reaction. Again to tailor down the rate constant to molecules produced per second we utilized the expression below.

$$K_{\text{degradation}} = \frac{\ln(2)}{t_{1/2}} = \frac{\ln(2)}{1800} = 3.85 \times 10^{-4} \text{ molecules per second degraded}$$

Rate of Protein Translation and Degradation

To estimate the protein synthesis constant and the protein degradation constant we again utilized a similar approach to that applied to the RNA paradigms. By investigating the database we discovered that the average rate of translation is 18 amino acids per second. To normalize the rate for a single molecule we utilized the following expression.

$$K_{\text{translation}} = \frac{[\text{Length of Protein}] \text{ aa}}{\frac{[\text{Rate of Translation}] \text{ aa}}{\text{second}}} = \frac{[\text{Length of Protein}]}{18} \text{ second}$$

To estimate the half-life of protein and thus calculate the rate constant for degradation assuming first-order kinetics we found that the average half-life for a protein was 60 minutes or 3600 seconds. To calculate the rate of protein degradation we utilized the following expression.

$$K_{\text{degradation}} = \frac{\ln(2)}{t_{1/2}} = \frac{\ln(2)}{3600} = 1.92 \times 10^{-4} \text{ molecules per second degraded}$$

Following the generations of these expressions there was a paradigm shift between each transcript and translation unit determine by the length of previous component thus creating variability among different bio bricks. Specific numbers for rate constants are presented in the model report included in the supplementary material.

Protein Interactions

Following generation of those concepts we wanted to quantify and model the rest of the processes described in table 1 of this document. To do so we lacked the statistical power of the database, since our parts interaction in the protein level were not highly characterized in the databases literature. Therefore, that embarked us in a journey to scavenge for specific variables that would be able to satisfy the differential equations described in the previous sections. Before starting the literature presentation and integration of the equations to make a completing model with output, we will briefly present the variable under investigation in the subsequent table.

Process	Variable under Investigation
Enzyme Driven Kinetics	K catalysis K complexion K dissociation
Protein-Protein Interactions	K complexion K dissociation
Diffusion Rates for Specific Molecules/Ions/ Compounds	K introduction K expulsion

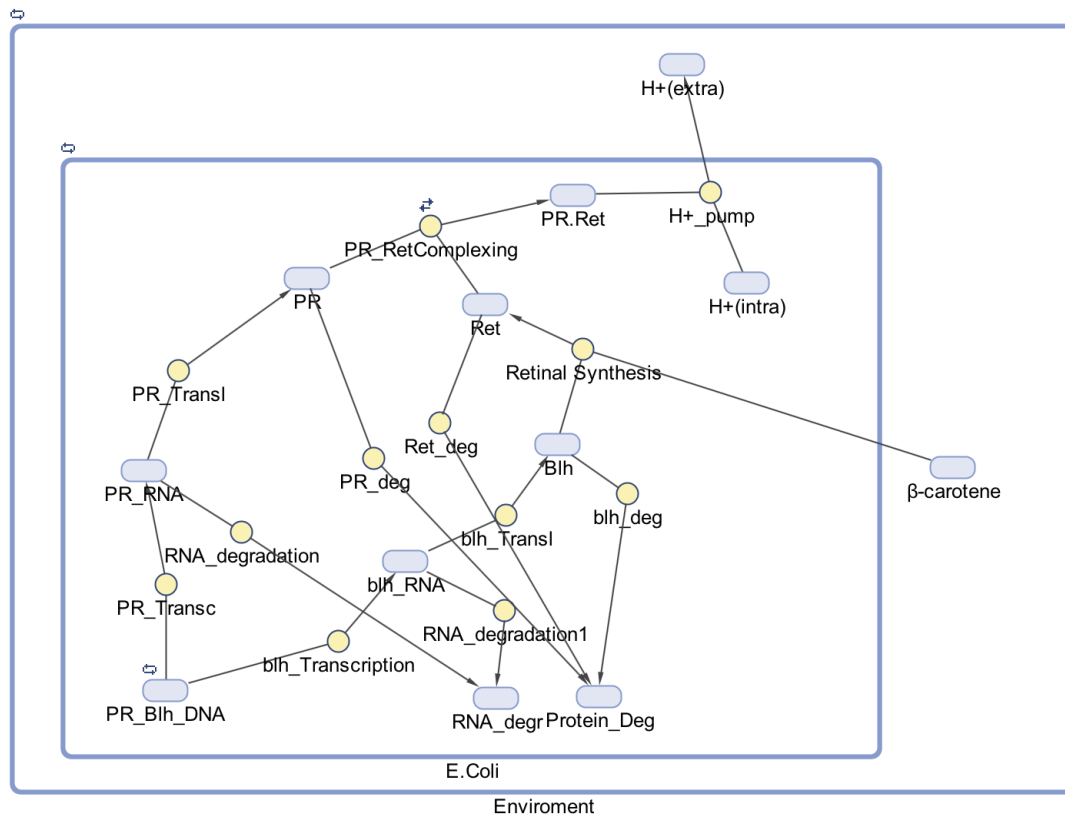
As we move through the specific model description literature we found to hold relevance to those variables that would complete the model will be provided for review.

Proteorhodopsin, Light-Driven Pump, Model

The first model we wanted to generate was related to the functionality of the bacterial proton light driven pump, Proteorhodopsin. The concept of in this system was that through induction of proton output generated by our plasmid constructs we would be able to sustain an electrolyte with higher conductivity and thus more current. This phenomenon would allow for increased efficiency in voltage generation.

As described in previous chapters of this project the main constructs utilized to optimize the electrolysis were those of PR (Proteorhodopsin) and Blh (Beta-carotene 15,15'-dioxygenase) in the form of plasmid DNA. The molecular interacting scenario involves the transcription of those nucleic acids into their corresponding mRNAs, followed by their translation by their ribosome. Once functional proteins have been generated this initiates the cascade that will eventually lead to an increased ATP production and proton pumping to the

extracellular environment. To form an active pump PR must bind to R (Retinol) and form an effective complex through protein-protein interaction. R is synthesized by the presence of the Blh enzyme and β -carotene, which is mediated by an enzyme driven reaction. Once R is synthesized effective complexion between PR and R leads to an active pump in the presence of light wavelength of $\lambda = 520$ nm. Activation of the pump leads to the efflux of proton to the environment, thus the electrolysis cell. Before starting this hypothetical endeavor we didn't know what to expect as an output of the functions generated from the principles set previously in this section. Here you can see the model diagram with all the bio bricks interacting.



Protein Synthesis

As described in the previous sections in order to model the formation of proteins from precursor DNA we utilized four ODE describing the transcription, translation, and degradation of both RNA and Protein. In order to determine the specific lengths of RNA in nucleotides and Protein in amino acids, we utilized the NCBI databases (<https://www.ncbi.nlm.nih.gov>) to acquire the transcript and the coding sequence of PR and Blh the components that undergo protein synthesis in this model. Then those lengths were utilized to calculate the rate constant as indicated in previous sections followed by expression generation that would allow for effective modeling of the processes. In the diagram above you can observe that transcription, translation and their degradation are included as separate species in order to allow for proper quantification of the degradation in the final output.

Retinal Biosynthesis

Being an enzyme catalyzed reaction retinal synthesis required us to investigate previous literature to seek the Kcatalysis constant. In this specific reaction we didn't require to account for any previous complex formation before the catalysis reaction since both precursors were supplied artificially. Retinal synthesis requires the enzyme Blh and β -carotene to be synthesized. Blh protein bioavailability was calculated over time with methods described previously. In the case of estimating the value of bioavailable β -carotene to a single E. Coli cells we assumed that the electrolysis cell would be populated 40 % with E. Coli, thus the volume occupied by all the E. Coli assuming plateau growth was given by this relationship.

$$Volume_{occupied\ by\ E.Coli} = Volume_{Electrolysis\ Cell} \times 0.4$$

$$E.Coli_{Electrolysis\ Cell} = \frac{Volume_{occupied\ by\ E.Coli}}{Volume_{E.Coli}}$$

Next, we assumed that experimentally an amount of concentration of β -carotene would be supplied to the electrolysis cell. Through conversion calculations we determined the amount of molecules of β -carotene present in the entirety of the electrolysis cell. Assuming equal distribution of molecules and E. Coli we calculated the amount of β -carotene to be 50 molecules per E. Coli utilizing this expression.

$$\beta - carotene\ molecules\ per\ E.Coli = \frac{\beta - carotene\ molecules}{E.Coli_{Electrolysis\ Cell}}$$

Next, we utilized our Bio Number database to determine the diffusion rate of β -carotene inside our E. Coli compartment. This extract pointed us to the right direction for proper modeling of diffusion "Diffusion coefficient for an "average" protein: in cytoplasm $D \approx 5-15\ \mu m^2/s \rightarrow \approx 10\ milliseconds$ to traverse an *E. coli* $\rightarrow \approx 10\ s$ ".

By determining the entry of β -carotene inside the cellular environment we moved on to model the synthesis of retinal from its precursor β -carotene catalyzed by the Blh enzyme we introduced. To do so we performed literature search to identify the unknown variable of Kcatalysis. Through our search several reaction kinetic experiments pointed us to values ranging from 0.1 to 0.45 per second for the catalysis rate (2,3). In effect our computational approach yielded us with realistic output for the bioavailability of Retinal inside the cell.

Proteorhodopsin Complex Formation and Proton Efflux

By computationally calculating the bioavailability of our major functional component we moved on to determine the ability of the model to predict proton efflux. The first computation we wanted to input into the model was the binding and dissociation of PR and R, a protein-protein interaction. In this paradigm the

variables that we were investigating were those of Kcomplexing and Kdissociation. Looking at the available literature we were amazed by the fact that there was no current characterization of reaction kinetics utilizing biological assays. In our search we were able to extract a publication that characterized the reaction light-cycle of Proteorhodopsin (4). The paper by Lanyi et al. was able to deduce that PR transitions through several structural intermediates that exist in equilibrium with a final structure that is related to the proton efflux of the complex. The experimental design was in brief a Gradient-Absorbance through time that would allow for quantitative measurement of the light-driven photochemical reaction. Reflecting back to Beer's Law we were able to deduce the relationship between the Absorbance and Concentration of PR utilizing this expression, thus providing us with a relatively strong estimating power about the reaction kinetics.

$$Absorbance = e \times b \times C$$

,where e stands for Molar absorptivity in L per mol per cm, b which stands for path length of sample in cm, and C the sample concentration.

In summation of the conclusions on the publication the experimenters generated time constants for both forward and reverse reaction rates presented below.

TABLE 1 The time constants of the transitions and the electrogenicities of the photocycle intermediates of the proteorhodopsin, measured at 20°C

Intermediate or transition	Forward reaction	Back-reaction	Relative electrogenicity
K			−0.0017
K to M ₁	43 ms	14 ms	
M ₁			−0.0085
M ₁ to M ₂	222 ms	–	
M ₂			−0.0073
M ₂ to N	0.53 ms	1.9 ms	
N			0.24
N to PR'	18.8 ms	119 ms	
PR'(O)			0.7
PR' to PR	153 ms	–	
PR			1

Here you can observe the time constants of the intermediates, along with the final forward reaction of PR with intracellular protons to promote proton efflux. In order to make this experimental values usable in our model we assumed the first order kinetics from transition of intermediate K to PR(O)'. Then we were able to calculate the reaction rate constant with the expression below.

$$t_{\frac{1}{2}} = \frac{\ln(2)}{k} \Leftrightarrow \tau \times \ln(2) = \frac{\ln(2)}{k} \Leftrightarrow k = \frac{1}{\tau}$$

Finally, by having calculated the rate constants we utilize the method of Cumulative and stepwise formation constants to generate a compound rate for the intermediates before the final active complex was formed (5). The final rate for the complex formation of PR with retinal was provided by this expression.

$$\beta_{forward} = K_{complexing\ formation}$$

$$\beta_{reverse} = K_{dissociation}$$

, where β is the cumulative constant for the reactions of $K \rightarrow PR(O)'$ and $PR(O)' \rightarrow M2$ and $M1 \rightarrow K$

Additionally, the rate for proton efflux was calculated to be,

$$K_{H+efflux} = \frac{1}{\tau} = \frac{1}{153 \times 10^{-3} \text{ second}} = 6.53 \text{ second}^{-1}$$

Finally, in order to calculate the intracellular H^+ free ions in a single E. Coli we utilized the following expression, assuming the pH of E. Coli would be 7.2

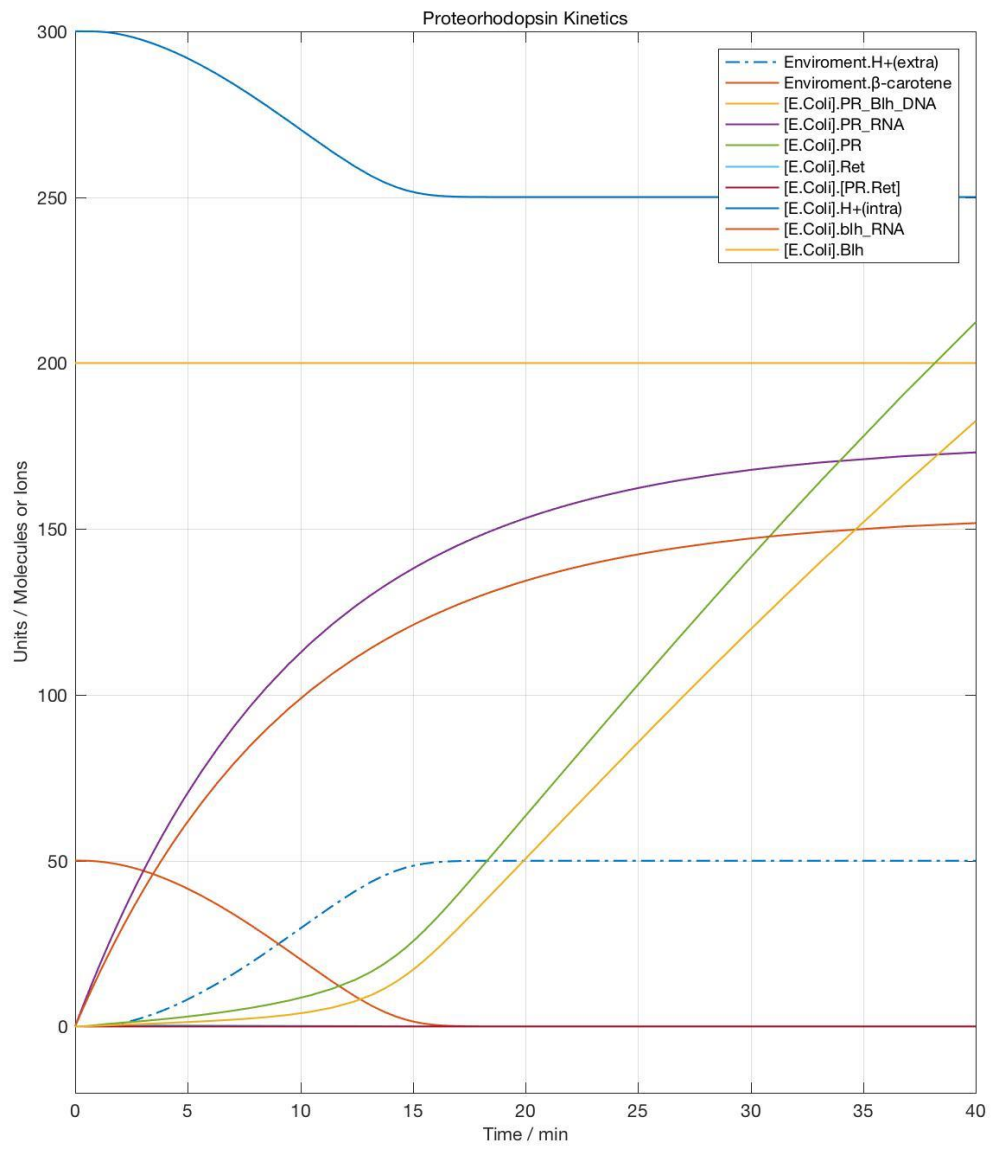
$$\begin{aligned} pH = -\log[H^+] &\Leftrightarrow [H^+] = 10^{-7.2} \Leftrightarrow 10^{-7.2} = \frac{N}{N_A \times V} \Leftrightarrow N \\ &= 10^{-7.2} \times N_A \times V \end{aligned}$$

, where N is the number of molecules, N_A is the Avogadro's number, V the volume of the cell

Performing this calculation we found out that if we actually utilized the output our model's output would be scrambled by the high order of magnitude and therefore just assumed a value of 300 bioavailable H^+ ions in the system.

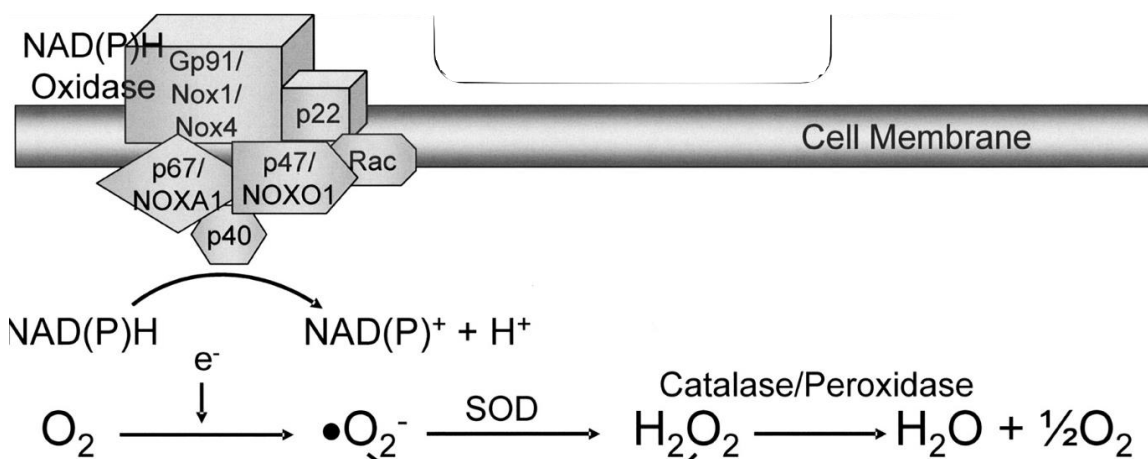
Model Output

In the figure "Proteorhodopsin Kinetics" we can see the output of the model created with the principles outlined in the previous section. The major output of the genetic circuit was the number of H^+ ions pumped outside of the cellular membrane. We can see from the plot of that in fact there is output of 50 H^+ ions outside the cell membrane, induced by activity of PR in a single E. Coli cell. This phenomenon is indicated by the dotted line plotting the change of H^+ ions over a single cell cycle. Therefore, compounding the experimental evidence discovered by other researchers, we were able to prove computationally that such a circuit would be able to increase the conductivity of the electrolysis solution, when we look at this system in isolation.



H₂O Forming NADH Oxidase Model

In order to model the second functional component of our project we utilized similar methodologies to those employed in the PR modeling. We started by cancelling out large secondary regulatory circuits that would make the task highly challenging for computation and research. Even if that was the case, we wanted to investigate the output of the reactions illustrated in the following figure produced by the literature (7).



Here we can see a simplified version of the NADH oxidase (Nox) pathway that converts NADH to NAD⁺, along with production of an electron. The electron in sequence increases the production of oxygen radicals that follow a biochemical reaction to be converted to water and half the initial oxygen. Therefore, this circuit is able to induce the desired anaerobic environment for optimization of the fuel cell's function. In this simplified model we tried to model this pathway by taking into account each conversion process and utilizing literature to computationally show that treatment of *E. Coli* with a Nox construct can induce anaerobic environments.

Protein Synthesis

As stated in previous section of the model we utilized the NCBI databases to generate the rate constants for the transcription of nucleic acids and the translation of mRNA depending on the length of transcript and translating mRNA. For degradation of both nucleic acids and protein we utilized the principal rates we speculated about in the foundation section.

NADH Oxidase Activity

In order to determine the rate of oxidation of NADH we run literature searcher to extract and utilize experimental rates for the reaction of NADH with Nox to produce NAD⁺, H⁺ and an electron (9,10). In our search we decided to speculate

from experimental results and utilize a value of $k_{\text{cat}} = 43.4 \text{ s}^{-1}$ for this enzyme driven reaction.

Oxygen Diffusion and Generation of Oxygen Radical

To calculate the rate of diffusion across membranes we utilized Fick's Law and values we assumed and gathered from databases, given by this relationship. We assumed that the diffusion rate of efflux would be 1/3 lower due to electromagnetic interactions inside the cell.

$$K_{\text{diffusion}} = D \times A \times \frac{\Delta P}{T}$$

, where D is the diffusion coefficient of the O₂, A is the surface area of the E. Coli membrane, ΔP the difference in partial pressure between extracellular and intracellular environment and T the thickness of the membrane.

In order to determine the rate of generation of oxygen radicals from the reaction of Oxygen with a free electron we scavenged the literature for related kinetic rate constants (11). Not being able to deduce a rate in molecule⁻¹ second⁻¹ from the literature we just speculated that the rate for oxygen radical formation would be 15 molecule⁻¹ second⁻¹.

Superoxide Dismutase Catalysis

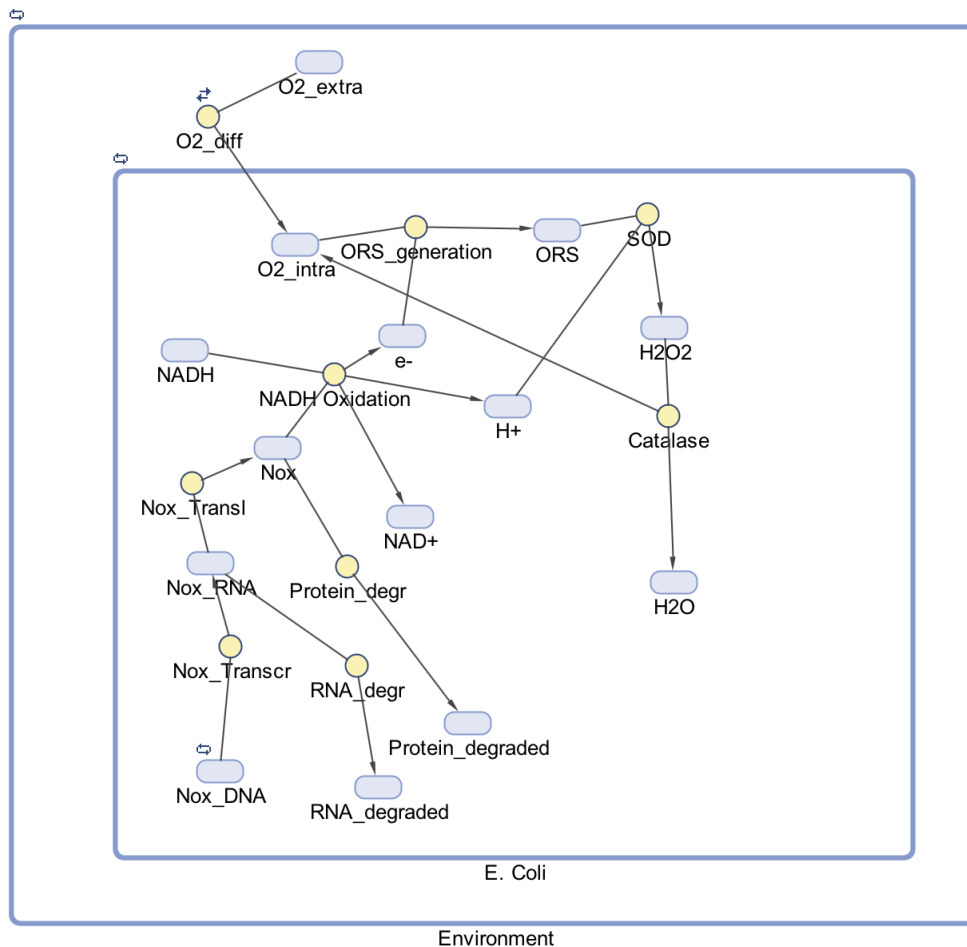
The next catalytic reaction we searched to find variables in the literature was that of the conversion of oxygen reactive species to peroxide, mediated by the enzyme Superoxide Dismutase (SOD). Running a literature search we speculated a rate of 200 molecule⁻¹ second⁻¹ (12).

Catalase Activity

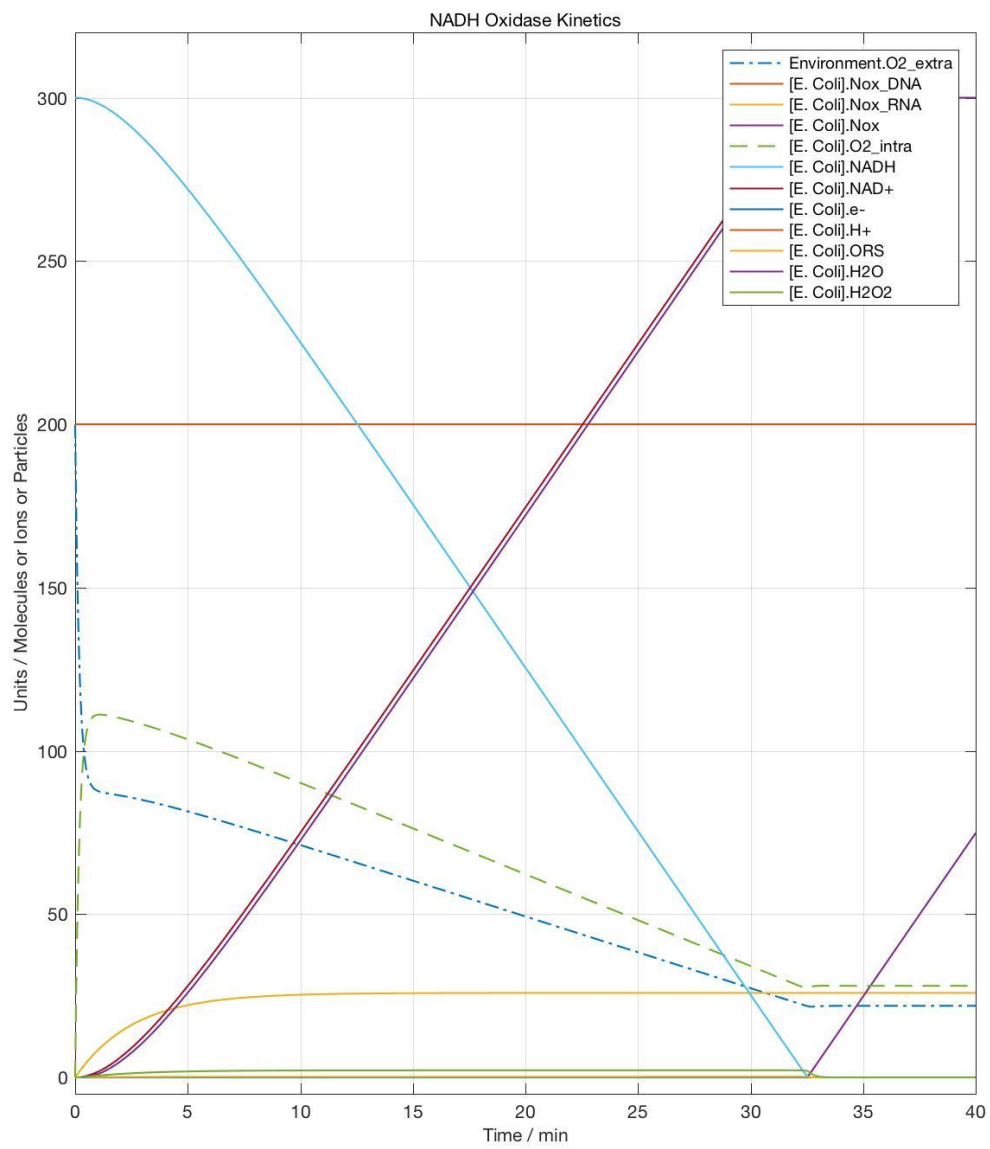
The final step of the anaerobic environment induce was the conversion of peroxide into water and half the molar ratio of oxygen introduced by the environment. Our search yielded a rate constant of 4.57 second⁻¹ as indicated in the literature (13).

Model Description and Output

In the following diagrams and figure you can observe the integration of all those pathways to generate a relatively simplistic and highly speculative model. In our understanding this circuit posed a highly challenging computational task, since multiple of its components interact with other cellular elements to produce an output. In summary you can observe the protein synthesis of Nox, which follows with the interaction of bioavailable NADH to generate electrons. Then those electrons will reduce the diffused oxygen, which in effect will be converted to peroxide by ORS, letting catalase finish the work with conversion of peroxide to water and oxygen, of a factor of 1/2 compared to the input oxygen.



By simulation of the model above, the following plot was generated for a cycle of single E. Coli. In the figure below you can see that by a speculation and extraction of experimental data from the literature our model was able to predict out hypothesis that this system at least in isolated computation would result in decreases environmental oxygen. This is shown by the blue dotted line that presents the levels of extracellular oxygen in comparison to the green dotted line that presents the levels of intracellular oxygen decreasing over the time period of a cell cycle in a single E. Coli cell. From this we can speculate that a population of E. Coli would decrease the oxygen in a closed system as our Microbial Fuel Cell, thus promoting the current circulation and increasing the efficiency of the voltage output.



Citations

- 1) "MATLAB." - MathWorks. N.p., n.d. Web. 15 Oct. 2016. <<https://www.mathworks.com/products/matlab/?requestedDomain=www.mathworks.com>>.
- 2) Ruch, S., Beyer, P., Ernst, H. and Al-Babili, S. (2005), Retinal biosynthesis in Eubacteria: *in vitro* characterization of a novel carotenoid oxygenase from *Synechocystis* sp. PCC 6803. *Molecular Microbiology*, 55: 1015–1024. doi:10.1111/j.1365-2958.2004.04460.x
- 3) Bchini, Raphaël, Vasilis Vasiliou, Guy Branlant, François Talfournier, and Sophie Rahuel-Clermont. "Retinoic Acid Biosynthesis Catalyzed by Retinal Dehydrogenases Relies on a Rate-limiting Conformational Transition Associated with Substrate Recognition." *Chemico-Biological Interactions* 202.1-3 (2013): 78-84. Web.
- 4) Bchini, Raphaël, Vasilis Vasiliou, Guy Branlant, François Talfournier, and Sophie Rahuel-Clermont. "Retinoic Acid Biosynthesis Catalyzed by Retinal Dehydrogenases Relies on a Rate-limiting Conformational Transition Associated with Substrate Recognition." *Chemico-Biological Interactions* 202.1-3 (2013): 78-84. Web.
- 5) Lancashire, Prof. Robert John. "Stability, Chelation and the Chelate Effect." *Stability, Chelation and the Chelate Effect*. N.p., n.d. Web. 15 Oct. 2016. <<http://wwwchem.uwimona.edu.jm/courses/chelate.html>>.
- 6) Bower, James M., and Hamid Bolouri. *Computational Modeling of Genetic and Biochemical Networks*. Cambridge, MA: MIT, 2001. Print.
- 7) Datla, S. R., and K. K. Griendling. "Reactive Oxygen Species, NADPH Oxidases, and Hypertension." *Hypertension* 56.3 (2010): 325-30. Web.
- 8) Wimpenny, Julian W. T., and Anne Firth. "Levels of Nicotinamide Adenine Dinucleotide and Reduced Nicotinamide Adenine Dinucleotide in Facultative Bacteria and the Effect of Oxygen." *Journal of Bacteriology* 111.1 (1972): 24–32. Print.
- 9) Shi, Xin-Chi, Ya-Nan Zou, Yong Chen, Cheng Zheng, Bing-Bing Li, Jia-Hui Xu, Xiao-Ning Shen, and Han-Jie Ying. "A Water-forming NADH Oxidase Regulates Metabolism in Anaerobic Fermentation." *Biotechnol Biofuels Biotechnology for Biofuels* 9.1 (2016): n. pag. Web.
- 10) Nowak, Claudia, Barbara Beer, André Pick, Teresa Roth, Petra Lommes, and Volker Sieber. "A Water-forming NADH Oxidase from *Lactobacillus Pentosus* Suitable for the Regeneration of Synthetic Biomimetic Cofactors." *Front. Microbiol. Frontiers in Microbiology* 6 (2015): n. pag. Web.
- 11) Song, Chaojie, and JiuJun Zhang. "Electrocatalytic Oxygen Reduction Reaction." *PEM Fuel Cell Electrocatalysts and Catalyst Layers* (n.d.): 89-134. Web.
- 12) Gray, B., and A. J. Carmichael. "Kinetics of Superoxide Scavenging by Dismutase Enzymes and Manganese Mimics Determined by Electron Spin Resonance." *Biochem. J. Biochemical Journal* 281.3 (1992): 795-802. Web.
- 13) Su, Chris, Meiyi Li, and TR. "Catalase Kinetics." *Catalase Kinetics Chris Su Meiyi Li TR* (n.d.): n. pag. MIT Press. MIT. Web. <<http://web.mit.edu/chris-su/Public/5310lab3.pdf>>.
- 14) Murray, Richard M. "Biomolecular Modeling." (n.d.): n. pag. *California Institute of Technology*. CALTECH CDS/BE, 26 Aug. 2009. Web. <http://www.cds.caltech.edu/~murray/books/AM08/pdf/bfsog-L1_modeling_26Aug09.pdf>.
- 15) "CHEM-5151 / ATOC-5151 - Atmospheric Chemistry." *CHEM-5151 / ATOC-5151 - Atmospheric Chemistry*. N.p., n.d. Web. 15 Oct. 2016. <<http://cires1.colorado.edu/jjimenez/AtmChem/>>.
- 16) Zhang, Ye-Wang, Manish Kumar Tiwari, Hui Gao, Saurabh Sudha Dhiman, Marimuthu Jeya, and Jung-Kul Lee. "Cloning and Characterization of a Thermostable H₂O-forming NADH

- Oxidase from *Lactobacillus Rhamnosus*." *Enzyme and Microbial Technology* 50.4-5 (2012): 255-62. Web.
- 17) "Reference Links for Key Numbers in Biology." *Reference Links for Key Numbers in Biology*. Harvard, n.d. Web. 15 Oct. 2016. <<http://bionumbers.hms.harvard.edu/KeyNumbers.aspx>>.
 - 18) "SimBiology® for Pharmacokinetic and Mechanistic Modeling." (n.d.): n. pag. *Mathworks*. Mathworks. Web. <<https://www.mathworks.com/discovery/supporting-docs/using-simBiology-for-pharmacokinetic-and-mechanistic-modeling.pdf>>.
 - 19) Balouri, Hamid. "Regulation of Gene Expression." *Encyclopedia of Molecular Pharmacology* (n.d.): 1063. *California Institute of Technology*. Caltech, Aug. 2008. Web. <http://www.its.caltech.edu/~hbolouri/Yale_Course_Slides.pdf>.